Leaf Hydraulic Architecture and Stomatal Conductance: A Functional Perspective[1][OPEN]

Fulton E. Rockwell[2] and N. Michele Holbrook

Department of Organismic and Evolutionary Biology, Harvard University, Cambridge, Massachusetts 02138

ORCID ID: 0000-0002-2527-6033 (F.E.R.).

The structure of leaf vasculature viewed over a broad phylogenetic scale from lycophytes to eudicots correlates with stomatal conductance, providing the basis for the hypothesis that increasing vein density drove the evolution of high fluxes in angiosperms. Yet, the relationship between vascular geometry and gas fluxes breaks down at finer phylogenetic scales. In this Update, we derive a simple one-dimensional model suitable for mapping the effects of three-dimensional vascular architecture and transport capacity onto an effective length for transport through the mesophyll. This approach allows us to explore notions of optimality in the hydraulics of reticulately veined leaves, which differ from the two-dimensional case. We then consider limits to stomatal conductance that may derive from genomic constraints on cell size and the role of mechanical advantage. We conclude that more mechanistic modeling of transpiration could help resolve the sensitivity of stomatal, genome, and vein density relationships to the phylogenetic scale of the study.

PATTERNS OF VASCULAR ARCHITECTURE IN RELATION TO STOMATAL CONDUCTANCE

Leaf vascular architecture has been described as a critical driver of the evolution of high leaf-level stomatal conductance over geologic time (Boyce et al., 2009; Brodribb and Feild, 2010; de Boer et al., 2012; Zwieniecki and Boyce, 2014a; McElwain et al., 2016). The theoretical justification for a focus on vascular pattern rests on the idea that a principal constraint on the supply of water to the stomata arises from the pathlength for transport through the mesophyll, a length strongly influenced by vascularization (Brodribb at al., 2007, 2010; Noblin et al., 2008; Boyce et al., 2009). The vascular trait most often adopted as a proxy for the effect of vascular pattern on transport efficiency is leaf vein density (D_v; linear vein distance per area; mm^{-1}).

A critical question arising in any investigation of vein density is the extent to which high vein density marks both a necessary and sufficient condition for high stomatal conductance. A necessary condition would support the hypothesis that the evolution of high vein densities in derived angiosperms removed a limiting constraint that continues to throttle stomatal conductance in extant ferns, gymnosperms, and basal angiosperms (Boyce et al., 2009; Brodribb et al., 2010; de Boer et al., 2012). A lack of sufficiency need not disturb this conclusion, although it would caution against the interpretation of vein density as a functional trait predictive of productivity. Clearly, the abilities of two different species growing in the same location to maintain a particular level of stomatal conductance may be limited by many factors besides leaf hydraulic conductance or vein density, including rooting depth (Sperry et al., 2002), leaf turgor loss point (minimum leaf water potential; Brodribb and Holbrook, 2003), and xylem cavitation resistance throughout the whole plant

ADVANCES

- We review recent work on the hypothesis that evolutionary changes in leaf vascularization have lifted an important constraint on maximum stomatal conductance in angiosperms relative to earlier diverging clades.
- Support for this hypothesis tends to be strong at coarse phylogenetic scales, but recently a number of studies have found a lack of support at finer scales.
- New leaf transport models account for both liquid and vapor water transport along the extravascular path in leaves, allowing evaluation of the importance of vascular and mesophyll material properties.
- Genome and cell size relationships, in conjunction with cell size coordination across vascular, mesophyll, epidermal, and stomatal tissues, provide an alternative source of nonhydraulic constraints on maximum stomatal conductance.

[1] This work was supported by the National Science Foundation (grant nos. IOS 1456836, IOS 1659915, and DMR 14-20570) and the Air Force Office of Sponsored Research (grant no. FA9550-09-1-0188).

[2] Address correspondence to frockwell@oeb.harvard.edu.

N.M.H. conceived the scope of the Update; F.E.R. performed the analyses; N.M.H. and F.E.R. wrote the article.

[OPEN] Articles can be viewed without a subscription.

www.plantphysiol.org/cgi/doi/10.1104/pp.17.00303

(Sperry and Love, 2015), and the ultimately limiting factor in any particular instance may be accompanied by an apparent overinvestment or underinvestment in vein density. Here, we focus on the common hypothesis that vein density tracks stomatal conductance, as, other things being equal, higher vein density should allow a larger liquid water flux and so higher transpiration rate that follow from greater stomatal aperture. In instances where vein density lacks predictive power for a leaf's ability to support a potential vapor flux and/or its hydraulic conductance, the question then becomes what other leaf characteristics explain the observed variation in the ability to supply water to a transpiring surface.

Support for the importance of vein density appears to be strongest over broad phylogenetic scales. Stevens (2001) summarizes the apparent linkages between phylogenetic patterns of vein density and the rise to ecological dominance of the angiosperms by noting that, prior to and for the first 30 million years after the appearance of angiosperms, fossil leaf D_v averaged 3 mm^{-1}, while angiosperm-type leaves with $D_v \sim 6$ mm^{-1} appeared ~100 million years ago, and 10 mm^{-1} and higher appeared after about 70 million years ago as CO_2 fell through the Cenozoic, a pattern corresponding to changes in D_v across extant ANITA grade, magnoliid, and eudicots, respectively (Boyce et al., 2009; Brodribb and Feild, 2010; Feild et al., 2011a, 2011b). From a functional perspective, over a similarly broad range of 19 ferns, conifers, and angiosperms, D_v has been shown to correlate with a measure of maximum operating stomatal conductance (g_s_op; measured under saturating light and a low vapor pressure deficit < 2 kPa; Boyce et al., 2009; McElwain et al., 2016).

However, within more phylogenetically restricted samplings or over narrower ranges of D_v, the relationship between stomatal conductance and vein density breaks down. McElwain et al. (2016) show a pattern of increasing g_s_op with D_v for a sample of 18 ferns, gymnosperms, and angiosperms, but the trend depends on the inclusion of four eudicots with $D_v >$ 6 mm^{-1} and does not appear to hold for the 14 taxa below that threshold. Gleason et al. (2015) report that, for 35 evergreen Australian angiosperms, there was no relationship between D_v and g_s_op over a range of D_v from ~6 to 18 mm^{-1} and a range of g_s_op from 0.05 to 0.7 mol m^{-2} s^{-1}; nor did D_v show any relationship with whole-leaf hydraulic conductance. Scoffoni et al. (2016) reported that, among 30 species of *Viburnum* grown in a common garden, major and minor vein densities explained less than 8% and 4% of the variation in maximum values of stomatal conductance (calculated from Supplemental Text S1). Thus, even as D_v produces tantalizing patterns across vascular plants, these finer scale analyses show that vein density alone cannot account for the mass balance between the transport of liquid into and vapor out of a leaf that must exist. Progress in understanding what other factors intermediate in the relationship between D_v and g_s_op would appear to require a more mechanistic approach.

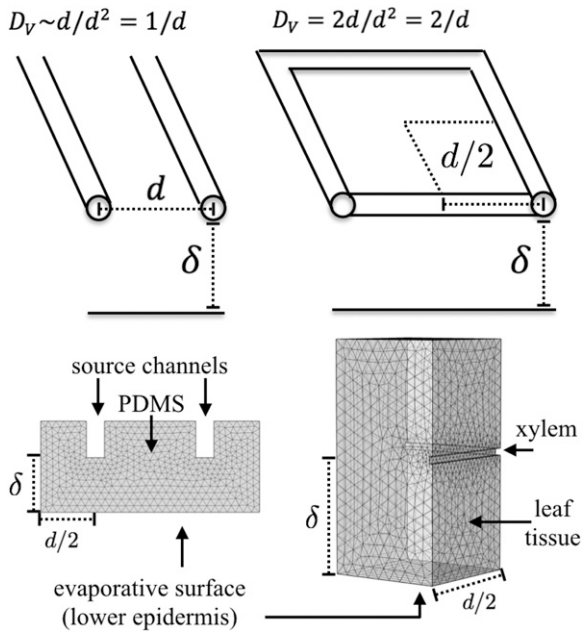

Figure 1. Diagram showing the theoretical relationship between vein density and intervein distance in parallel (2D) and reticulate (3D) vein geometries and the finite element domains used in the simulations of the Noblin et al. (2008) experiments (2D PDMS) and for transport in a quarter section (by symmetry) of an areole through the thickness of a hypostomatous leaf. For the 2D case, by symmetry, the domain of analysis need only encompass half the channel and a width *d*/2; here, we show larger domains for the purposes of illustrating the effects of channel density. Note that the 2D PDMS model system does not have a region analogous to the palisade tissue in a leaf.

OPTIMAL VASCULAR NETWORKS: AN INNOVATION UNIQUE TO ANGIOSPERMS?

Before turning to the challenges inherent in a mechanistic description, we will first try to retain the idea that the critical effect of the vascular network lies in how it structures mesophyll hydraulic conductance. Doing so requires addressing a major deficiency of D_v as a proxy for hydraulic transport capacity: that it fails to capture the effect of vein-to-lower epidermis distance (δ) on the pathlength of transpiration through the mesophyll (Brodribb et al., 2007). Noblin et al. (2008) showed that the ratio of intervein distance d (proportional to $1/D_v$; Fig. 1) to δ controlled the magnitude of the flux of water through an artificial leaf constructed of PDMS (polydimethylsiloxane). In this system, as channel density increased (i.e. d went to zero), the gradient driving water transport through the PDMS became increasingly one-dimensional (1D; parallel to the transpiring surface; Fig. 2, A and B). In the limit $d = 0$ (i.e. where the channels merge into a single continuous plane of water), transpiration reaches a maximum (Fig. 2C), and the pathlength for flow from the channels to the transpiring surface is just δ. In the absence of a true mathematical optimum along the smoothly increasing response, Noblin et al. (2008) developed a

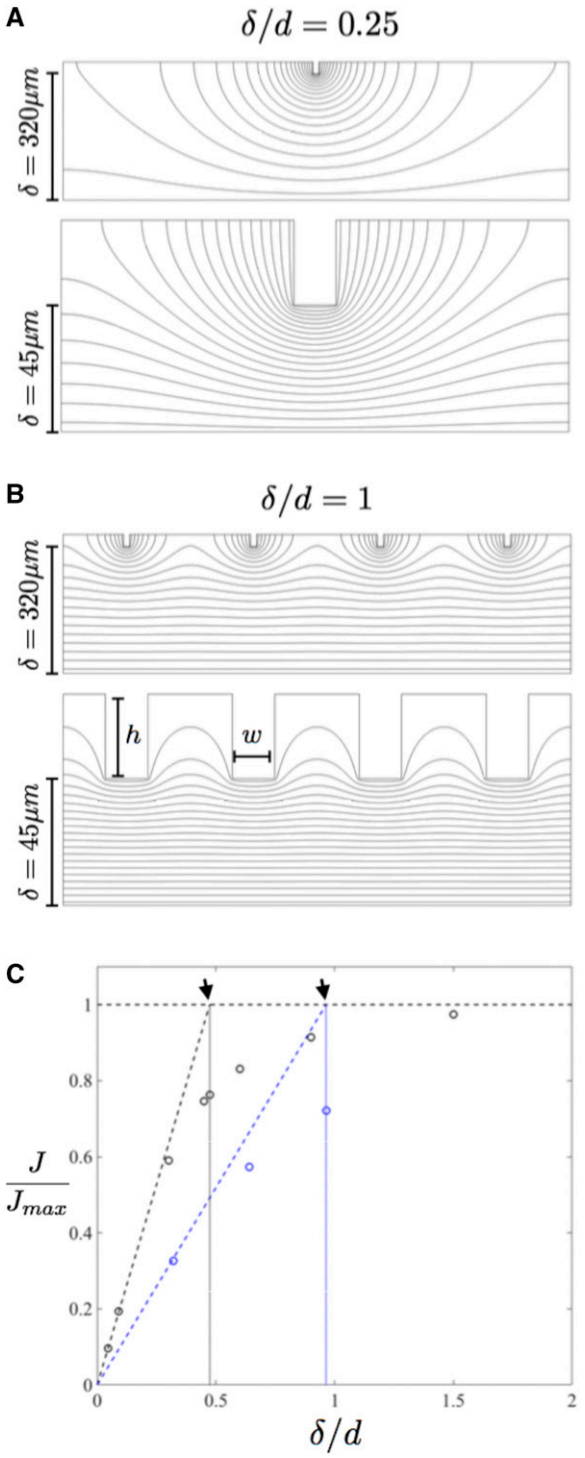

Figure 2. Effects of channel (xylem) size and spacing on the 2D flux of water to a transpiring surface. A, Contour plots of the gradient in the driving force for the water flux through a 2D domain for a thickness-to-intervein distance ratio $\delta/d = 0.25$ at two different thicknesses δ. B, The same simulations as in A but with $\delta/d = 1$; note that the channel size $h \times w$ is the same across all four simulations in A and B. As δ/d and channel size relative to δ increase, the contours become more parallel to the transpiring surface, such that the flux of water (normal to the contours) becomes more unidirectional (1D). C, Normalized 3D transpiring flux as a function of δ/d and channel (xylem) size relative to thickness; blue circles are for the channel size-to-thickness relationship obtained when $\delta = 320\ \mu m$, and black circles are for $\delta = 45\ \mu m$. J_{max} is the fully 1D flux obtained through a given thickness δ as δ/d becomes large. Dashed lines are for the approximate solutions of Noblin et al. (2008) in the limits of high and low δ/d: the intersection of these solutions (arrows) identifies the optimal δ/d (dotted line to the ordinal axis) and flux at which the flow transitions from approximately 2D to approximately 1D behavior.

rule based on the intersection of linear fits to analytic expressions for the limiting cases of channel density approaching zero and infinity (Fig. 2C). The authors proposed that an optimal channel (vein) density for a given thickness occurs at the intersection of the linear fits, typically at $d/\delta \sim 1$. This value was considered to mark the transition from a predominantly two-dimensional (2D) to 1D behavior of the flux and the point at which diminishing returns in vein density accelerated.

Applying this analysis to leaves, Zwieniecki and Boyce (2014a) found a mean d/δ for core eudicots of 1.4 (n = 39), versus 1.9 (n = 8) for Magnoliales + Laurales and 2.7 (n = 4) for ANITA-grade basal angiosperms, while conifers had a mean of 4.7 (n = 7) and leptosporangiate ferns had a mean of 5 (n = 27). Basal monocots had a mean of 3 (n = 6), while more derived monocots had a mean d/δ of 1.3 (n = 5). The interpretation provided by the authors was that optimal vasculature with a $d/\delta \sim 1$ evolved independently in the magnoliids, monocots, and eudicots. Yet, the overall distribution of d/δ appears to be quite similar to that of vein density (Boyce et al., 2009), raising the question of whether adding consideration of the thickness δ, while producing interesting theoretical developments, significantly improved our understanding of leaf-level hydraulic limitation of stomatal conductance (g_s).

Moreover, revisiting the original analysis of Noblin et al. (2008) raises questions concerning the application of the theory and the generality of an optimum occurring for all systems at $d/\delta \sim 1$. In fact, the original analysis showed that the intersection of linear fits varies with δ for a given channel size, such that the optimum occurred at $d/\delta \sim 1$ for a PDMS gel with $\delta = 320\ \mu$m but at a wider spacing of $d/\delta \sim 2$ for $\delta = 45\ \mu$m (Fig. 2C). The full rule for optimal d/δ with channels of height h and width w was given as,

$$\frac{d}{\delta} = \frac{\pi}{\ln\left((\delta + h)\Big/\sqrt{2wh/\pi}\right)}. \quad (1)$$

The optimum d/δ, therefore, itself is a function of a ratio of channel size to thickness δ, such that, for the same thickness, greater channel size would permit wider vein spacings to achieve the same flux. Equating the cross section of the aggregate of minor vein xylem to a square channel with sides equal to $2a$, the above rule becomes,

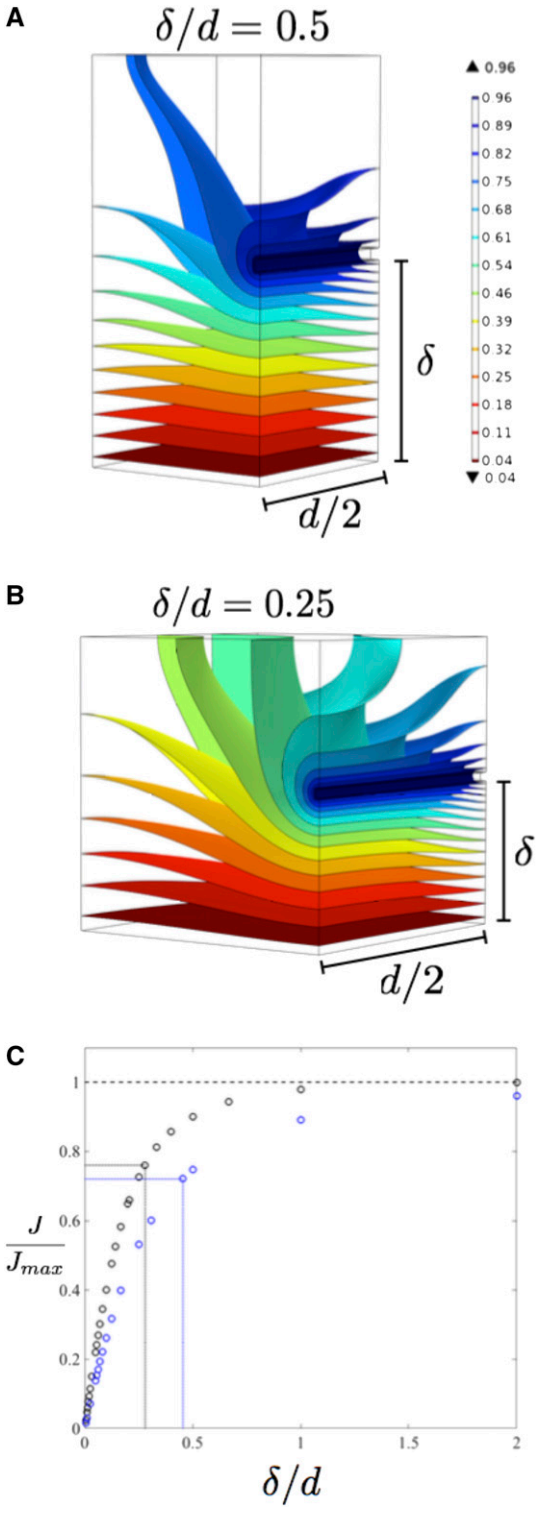

Figure 3. Effects of channel (xylem) size and spacing on the 3D flux of water in a quarter section of an areole. A, Isosurfaces of the normalized water potential (xylem = 1, lower epidermis = 0) induced by transpiration from the lower surface, for $\delta/d = 0.5$, with the same channel (xylem) size-to-thickness relationship as for the $\delta = 320$ μm simulations in Figure 2. B, The same simulation as in A, but for $\delta/d = 0.25$. As δ/d increases, the isosurfaces become planes normal to the transpiring surface, and the flux becomes more 1D. C, Normalized 3D transpiring flux as a function of δ/d and channel (xylem) size relative to thickness; blue circles are for the channel size-to-thickness relationship obtained in the 2D simulation (Fig. 2) when $\delta = 320$ μm, and black circles are for $\delta = 45$ μm. J_{max} is the fully 1D flux obtained through a given thickness δ as δ/d becomes large. For 3D areoles with the same channel size-to-thickness relationships, the optimal fluxes of the 2D cases (dotted lines) occur at half the δ/d values of the 2D cases (i.e. at wider vein spacing).

$$\frac{d}{\delta} = \frac{\pi}{\ln\left((\delta/a + 1)\Big/2\sqrt{2/\pi}\right)}. \quad (2)$$

For a sampling of 19 temperate woody angiosperms with δ/a ranging from 8 to 17 (Wylie, 1939; Rockwell et al., 2014c), the optimum predicted by Equation 2 occurs at d/δ from 1.3 to 1.7, while for ginkgo (*Ginkgo biloba*), a δ/a of 6 yields an optimum at about 2 (Leigh et al., 2011). Gymnosperms and some ferns, whose vascular bundles often contain large masses of tracheids relative to angiosperm minor veination, may then be less underbuilt in vein density than the $d/\delta \sim 1$ rule suggests.

Furthermore, accounting for the three-dimensional (3D) mesophyll geometry of reticulate (net) venation (Fig. 1) also shifts the optimum d/δ, as the 3D flux responds differently to d/δ than in the 2D (parallel vein) system (Figs. 2 and 3). For the equivalent δ/a to the 2D simulations of Figure 2 (i.e. such that Eq. 1 = Eq. 2), the flux approaches its maximum at higher values of d/δ (so wider vein spacings) than in the 2D case by about a factor of 2 (Figs. 2C and 3C), which may be explained by the fact that ideal reticulate veins have twice the vein density as parallel veins with the same d. In the absence of an analytic theory for the limiting cases in 3D geometry that would allow us to follow the procedure of Noblin for identifying the optimum d/δ, we instead simply note that the optimum fluxes of the 2D studies (0.76 and 0.74 of the maximum flux) now occur at d/δ values of 2 to 3 in the 3D analyses (Fig. 3C). For the range of δ/a for temperate woody angiosperms given above, an optimal flux of 0.75 of the maximum picks out a similar range of d/δ (2.25–3.25), and in this view, the eudicots sampled by Zwieniecki and Boyce (2014a) appear, from a hydraulic perspective, overbuilt. It is important to keep in mind, however, that, in the absence of a cost function, there is no clear functional basis for choosing precisely where along a smoothly diminishing curve of returns on investment in d a leaf should fall. If neither D_v nor d/δ can be counted as reliable proxies, then it seems inescapable that to make progress in understanding hydraulic limitations of stomatal conductance at the leaf level requires a physical model of the entire flow path.

MODELING THE CONTRIBUTIONS OF THE VASCULATURE AND MESOPHYLL TO LEAF HYDRAULICS

A useful empirical idea that emerges from the above analysis, perhaps more useful for our purpose than that of a theoretical optimum vein spacing, is that of an

effective length for transport from a channel (or vein) to a transpiring surface. As the interchannel distance approaches the channel width, we have seen that the gradients become increasingly parallel to the transpiring surface, and the flux that follows the streamlines normal to the gradients fits a 1D description of transport from source to sink over a distance δ. As d/δ falls and intervein distances increase, the gradients and flux become increasingly 2D (or, for areoles, 3D) and the flux falls as the average distance traveled by water molecules through the resistive medium (PDMS, mesophyll) increases. Thus, for any value of d/δ, there exists an effective length that maps the flux of the multidimensional system to an effective 1D form of transport between two points separated by that length. We can then use this idea to relate transpirational water loss from a leaf to internal water transport from the petiole to the stomata.

In steady state, mass balance requires,

$$g_T\Delta\chi = E = K\Delta\psi;\;\; K = \left[K_x^{-1} + K_m^{-1}\right]^{-1};\;\; g_T = \left[g_s^{-1} + g_b^{-1}\right]^{-1}, \tag{3}$$

where g_T, g_s, and g_b are the total, stomatal, and boundary layer conductances, $\Delta\chi$ is the leaf -to-air water vapor mole fraction difference, K is an effective leaf hydraulic conductance, K_x is the xylem conductance to the vascular-mesophyll interface, K_m is the effective hydraulic conductance of the mesophyll (defined here broadly as the living cells outside the xylem) from the veins to the stomata, and $\Delta\psi$ is the gradient in water potential (N.B., using water potential for the driving force in the xylem, rather than explicitly writing out the pressure and gravitational terms, is justified within the xylem because the reflection coefficient for solute transport is zero). Note that $\Delta\psi$ addresses the stem-petiole junction to the transpiring surface (e.g. the lower epidermis for a hypostomatous leaf) water potential difference, and not the stem-petiole junction to the average transpiring leaf water potential difference, such that K_m is not equivalent to the K_{ox} (outside xylem conductance) defined by Scoffoni et al. (2016). Similarly, K is not equivalent to K_{leaf} (Sack and Holbrook, 2006).

Based on an analysis of 3D flow in the internal leaf geometry of 19 woody temperate angiosperms (d/δ ranging from 1 to 4 and δ/a ranging from 8 to 17; Rockwell et al., 2014c), the relationship between K, the source water potential ψ_s (e.g. covered leaf potential for the stem-petiole junction for intact leaves, or the water reservoir for detached leaves), the average transpiring leaf water potential ($\langle\psi\rangle$) as measured by the pressure chamber, and the transpiring flux E, is given by (Supplemental Text S1),

$$K = E\left(\frac{1-\phi}{\psi_s - \langle\psi\rangle}\right). \tag{4}$$

The factor $1-\phi$, which can be predicted for a leaf with knowledge of δ, d, and a and the location of the plane of the vasculature vp, can be thought of as rescaling an observed source-to-leaf average water potential difference to the actual difference driving the flux from the source to the lower epidermis. The lower epidermis may be taken as the location where the leaf water vapor mole fraction is defined based on leaf thermocouple measurements with a gas-exchange system or porometer, with only a minimal (and correctable) error due to the neglect (in gas-exchange system calculations) of water potential effects on the water vapor mole fraction (Nobel, 2005; Rockwell et al., 2014a). For the 19 species described by Rockwell et al. (2014c), ϕ ranged from 0.76 to 0.53, such that K may be expected to be lower than K_{leaf} by a factor of 2 to 4 depending on leaf anatomy, as might be expected given the difference in pathlength represented by the two conductances. For a hypostomatous leaf, the effect of anatomy is that the greater the proportion of palisade tissue and the smaller the d/δ, the more average leaf water potential will be weighted toward the water potential at the xylem-mesophyll interface and the more K_{leaf} will be higher than K (Supplemental Text S1).

The use of Equation 4 should be guided by a couple of caveats. First, it is an approximate form that requires that K_x not be severely impaired by cavitation: the more general form cannot be solved algebraically for K and requires numeric evaluation (Supplemental Text S1). Second, the defined K is an effective leaf hydraulic conductance in that the driving force is taken as a water potential difference, but part of the flux it explains is contributed by nonisothermal vapor diffusion. This is not an issue unless the goal is to relate K to purely hydraulic properties such as cell permeability, in which case the true hydraulic conductivity of the mesophyll must be sought with a model that explicitly accounts for vapor transport (Rockwell et al., 2014a; Buckley et al., 2017).

For the purpose of interspecific comparisons of the efficiency with which different leaves can supply transpirational losses of water, the K of Equation 4 may be useful. For common garden conditions and similar growth forms, variation in $\Delta\Psi/\Delta\chi$ may be small enough that, by Equation 3, g_T is proportional to K across taxa. The first component of K, xylem conductance K_x, can then be estimated by steady-state vein-cutting experiments (Scoffoni et al., 2016). By definition, the second component can be written $K_m \equiv k_m/L_m$, a relation that decomposes K_m into an effective hydraulic conductivity of the mesophyll k_m and an effective length for transport L_m. Based on the results of Rockwell et al. (2014c) for the anatomy of 19 woody temperate angiosperms (Wylie, 1939), the effective distance through the mesophyll is well described (i.e. resulting in differences from the numerically simulated 3D flux of less than 2%) by,

$$L_m \equiv 0.69\delta + 0.36\sqrt{\delta^2 + (d/2)^2}. \tag{5}$$

This effective pathlength is a function of δ and the hypotenuse of the triangle formed by δ and $d/2$ (for

derivation, see Supplemental Text S1), the latter similar to the effective mesophyll distance d_m adopted by Brodribb et al. (2007). Note that, with these numerical coefficients, the effective pathlength slightly exceeds δ when $d/2 = 0$, a nonphysical result likely due to the fact that this is a limiting case outside the range of real data.

As the vascular and mesophyll paths are in series in a 1D mathematical form, it is helpful to work in terms of resistance rather than conductance. The K of Equations 3 and 4 is then written in terms of its reciprocal resistance ($R \equiv 1/K$), and the hydraulic conductivity of the mesophyll is written in terms of its reciprocal resistivity ($1/k_m \equiv r_m$), while K_x is converted into the vascular resistivity per areole vein length, r_V, by dividing by the vein density D_V ($K_x/D_V = 1/r_V$). As we wish to work in terms of intervein distance rather than density, we note that, for ideal squares of closed venation, the reciprocal of vein density is half the intervein distance (i.e. areole half-width), or $D_V = 2/d$ (Fig. 1). However, Brodribb and Feild (2010) report that, for angiosperms, the relation is closer to $D_V = 1.3/d$. To account for such nonideality, we introduce a scale factor s that varies from 1 to ~1.5 ($s = 1$ if d is observed directly, as we will generally assume here) and, for convenience, define the half-intervein distance $\omega \equiv d/2$, to write $R_x = s\omega r_V$. The total resistance to water transport from petiole to lower epidermis is then,

$$R = s\omega r_V + r_m\left(0.69\delta + 0.36\sqrt{\delta^2 + \omega^2}\right). \quad (6)$$

The change in total leaf resistance R for a change in ω is then evaluated as,

$$\frac{\partial R}{\partial \omega} = sr_V + 0.36r_m\left(1 + \frac{\delta^2}{\omega^2}\right)^{-1/2}. \quad (7)$$

Considering $\partial R/\partial\omega$, we see that there are two mechanisms by which adding more veins reduces R: the r_V term captures the effect of increasing the vascular supply per unit leaf area, while the r_m term describes the effect of a change in the pathlength through the mesophyll. An efficient ratio of r_m to r_V with respect to investment in veins is represented by a value that produces equal reductions due to pathlength and vascular supply effects. We can find such a target r_m/r_V for any ω/δ by setting the two terms in Equation 7 equal and solving for r_m/r_V:

$$\frac{r_m}{r_V} = \frac{s}{0.36}\left(1 + \frac{\delta^2}{\omega^2}\right)^{1/2}. \quad (8)$$

For a range of optimal ω/δ of 1 to 1.5 (i.e. $d/\delta \sim 2$ to 3, with $s = 1$) the values of r_m/r_V that result in equal vascular and mesophyll pathlength contributions range from ~3 to 4. Expressing this result in terms of the balance of vascular to mesophyll hydraulic resistance, an R_m/R_x of 3 to 5 represents a balance that attains equal contributions to the reduction of R from pathlength and vascular supply effects for a given extra investment in vein density.

This result is quite different from the well-known result for efficiently minimizing the total resistance of two resistors in series, which says that an efficient allocation of resources should lead to the two resistances being equal (assuming equal costs; Horowitz and Hill, 1989), an outcome that is close to the balance of lumen and end wall vascular resistance (Sperry et al., 2005). Imposing the Ohm's law result that $R_m = R_x$ on the terms in Equation 6, and ω/δ of 1 to 1.5 (with $s = 1$) results in an $r_m/r_V \sim 1$ (0.8–1.1). In this regime, marginal changes in vein density affect R predominantly through vascular supply, with the effect of changes in pathlength through the mesophyll relatively weak, and in that sense individual vascular bundles are underbuilt for the given vein density and mesophyll resistivity. Rather than attempting to infer which rule for r_m/r_V is best, given that relative costs remain a huge uncertainty for such an assessment, it is probably best to think of the above rules as describing a parameter space toward which selection for efficient reductions in resistance might lead.

THE IMPACT OF VASCULAR VERSUS MESOPHYLL HYDRAULICS: NORTHERN RED OAK AND GINKGO

For the sake of a concrete example, we consider northern red oak (*Quercus rubra*), a typical woody temperate eudicot in terms of vein density and d/δ (Zwieniecki and Boyce, 2014a). We previously developed a model of leaf cells and airspace as a composite porous medium with local equilibrium assumed between cells (liquid) and air (vapor; Rockwell et al., 2014a). We then used the same scaling idea that led to Equation 5 to map a 1D analytic solution of the two-phase coupled heat and mass transport problem to the 3D geometry of red oak leaves (Fig. 4, A and B). Solving the model in the context of an energy balance for a 262-μm-thick oak leaf under a photosynthetic photon flux density of 1,700 μmol m^{-2} s^{-1}, with the hydraulic resistivity r_m estimated from rehydration kinetics and accounting explicitly for vapor transport, predicted the average transpiring leaf water potentials of five leaves to within the typical error of the pressure bomb ($\pm$0.034 MPa; Rockwell et al., 2014a). For these leaves, K_{leaf}, defined conventionally as $E/(\Psi_s - \langle\Psi\rangle)$ (Sack and Holbrook, 2006), was 13 mmol m^{-2} MPa^{-1} s^{-1}, while K, defined by Equation 4, was 3.6 mmol m^{-2} MPa^{-1} s^{-1} (Supplemental Text S1).

Here, we show that the scaled 1D solution for the coupled heat and mass transport reproduces the results of the simulation of coupled heat and mass transport in the full 3D geometry (Fig. 4, C–G). There was no difference between the 1D and 3D solutions for the proportion of evaporation occurring in different regions (percentages in Fig. 4B); however, in the 3D analysis, it was possible to decompose the 1D prediction of 21% of evaporation occurring at the perivascular plane into

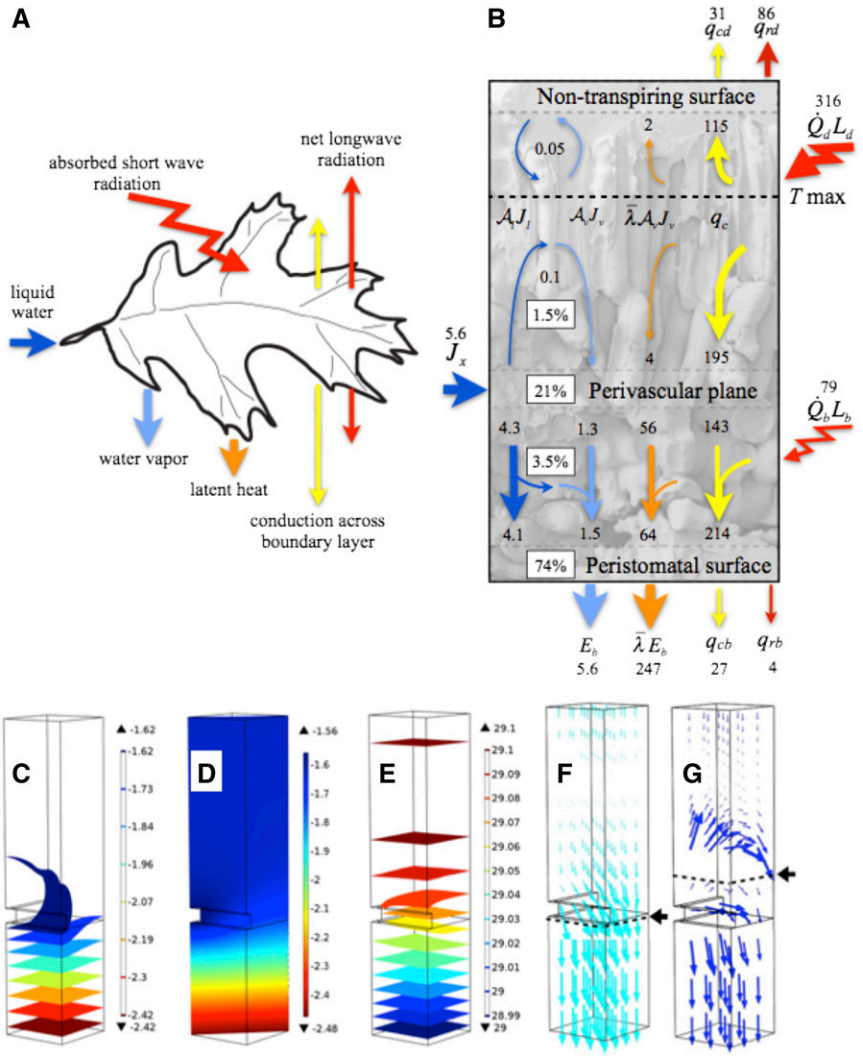

Figure 4. Scaling water transport in leaves as a function of leaf architecture and energy balance from 3D simulations to 1D representations. A, Fluxes contributing to leaf energy balance. B, 1D model results for a red oak leaf with internal and external fluxes of water molecules (mmol m^{-2} s^{-1}) as liquid (dark blue) and vapor (light blue) as well as energy (J m^{-2} s^{-1}) by conduction (yellow), latent heat (orange), and radiation (red); percentages are for the amount of *E* evaporating in different zones of the leaf (Rockwell et al., 2014a). C to G, Validation of the 1D model spatial results by a 3D simulation in a quarter section of an areole bounded on two sides by xylem (groove). C and D, Isosurfaces (C) and slice (D) for the water potential field, with color scales in MPa. E, Temperature isosurfaces, with Celsius color scale. F and G, Internal fluxes of water vapor (F) and liquid water (G) proportional to arrow length and size. To aid visualization, fluxes above the dotted line at the black arrows were magnified 10-fold for vapor and 20-fold for liquid relative to the fluxes below.

6.5% occurring from the veins themselves and 14.5% occurring at the palisade-to-spongy transition, consistent with the results of Buckley et al. (2017). Average water potentials of the 1D and 3D solutions for the upper palisade, vascular plane, spongy mesophyll, and lower epidermis of the leaf were within 2% (~0.03 MPa) of each other. These results demonstrate that the rescaling approach for mapping 1D mathematics to 3D problems works for both isothermal and nonisothermal cases, with the caveat discussed above that one must keep track of whether the modeled conductances and conductivities are effective (inclusive of vapor transport) or true hydraulic properties (accounting for liquid flow only).

For red oak and a definition of r_m that includes the effect of vapor transport, we estimate an r_m/r_V of 2.6 and $R_m/R_x = 4.8$ (Rockwell et al., 2014a). These experimental estimates imply that r_m/r_V falls about midway between the value of 4.5 predicted by the equal contributions to the $\partial R/\partial\omega$ idea in Equation 8 (with $\omega/\delta = 0.78$ and s = 1) and the value of 0.7 that would be predicted for oak by the Ohm's law equal resistance target. For red oak, vein spacing is already tight enough that an increase in D_v would reduce total leaf *R* more through vascular supply than mesophyll pathlength effects on R_m, which, for oak, is the dominant component of *R*.

By comparison, for the parallel-veined broad-leaf gymnosperm ginkgo, with a ω/δ of 2.33, more than twice the optimal $d/\delta = 2$ for parallel veins of this size given by the Noblin analysis, we have estimated an r_m/r_V ($s = 1$) of 5.7 (Rockwell, 2010; Leigh et al., 2011). As r_m for ginkgo is about half that of oak (note that, for ginkgo, r_m does not include the effect of temperature on vapor movement, which would lower it further), r_V for ginkgo is ~4 times lower than for oak. That is, ginkgo veins can supply more water per unit vein length than oak, even as, due to the difference in vein density, its vascular resistance per unit leaf area R_x is three times that of oak. Thus, relative to oak, gingko appears to have driven down total leaf *R* by increasing the number or diameter of the tracheary elements in each vein to a much greater extent, even though it would presumably

have realized much larger marginal reductions in R by reducing d and shortening the mesophyll pathlength.

That ginkgo seems to have overinvested in driving down r_V, rather than decreasing d, could be explained if the construction and opportunity costs (i.e. space consumed that might otherwise contain photosynthetic mesophyll) of nonxylem components in their large (relative to angiosperm minor venation) vascular bundles are high relative to the marginal benefits to assimilation of increasing vein number. The example of ginkgo then begs the general question of why gymnosperms and ferns do not simply reduce the size of their vascular bundles and simultaneously increase their density. One hypothesis is that the evolution of vessels in angiosperms increased the intrinsic efficiency of their tracheary elements, allowing them to reduce the number of xylem conduits in, and overall size of, their vascular bundles and increase their density: subsequent independent reductions of scalariform perforation plates to simple perforation plates in the primary xylem of more derived monocots, magnoliids, and eudicots then led to further increases in efficiency to allow high D_v values greater than 15 mm^{-1} (Feild and Brodribb, 2013). While this hypothesis could explain trends in D_v between vessel less basal angiosperms, ferns, lycophytes, and cycads (which all have homogenous pit membranes and tracheids) and more derived angiosperm taxa, the idea that vessel-based xylem has a higher hydraulic conductivity than tracheid-based xylem of the same area and average conduit diameter does not hold for tracheids with margo-torus pitting, as in conifers and ginkgo (Pittermann et al., 2005). Ginkgo tracheid diameters (10–15 μm; Leigh et al., 2011) overlap with midrib vessel diameter vessels in *Viburnum* spp. (9–18 μm; Scoffoni et al., 2016), and minor vein tracheary element diameters in red oak are in the range of tracheid diameters in *Taxus baccata* needles and *Pseudotsuga menziesii* fine branchlets (5–10 μm; Woodruff et al., 2008; Zhang et al., 2014, 2016). While a more systematic analysis than these ad hoc comparisons is required to draw any firm conclusions, we can say, based on Pittermann et al. (2005), that replacing the conduits in an oak minor vein with conifer-type tracheids of the same diameter would only increase the resistivity by about 20%, a loss that could be offset by an increase in tracheid diameter of only 5%. Therefore, it seems unlikely that conifers and ginkgo are constrained from achieving high D_v by the intrinsic resistivity of their xylem.

Indeed, some broad-leaf conifer taxa have evolved a way to achieve an intervein distance of effectively zero. For example, *Podocarpus grayi* produces a laminate leaf with a single vein by radially transporting water through accessory transfusion tissue, an almost continuous layer of extravascular (i.e. outside of a vein) tracheids that irrigate the midplane of the leaf (Brodribb and Holbrook, 2005). Nevertheless, g_s for this taxa is only ~50 mmol m^{-2} s^{-1} (Brodribb et al., 2005), so if one accepts that accessory transfusion tissue is functionally equivalent to intrusive veinlets in angiosperms, something besides D_v must be limiting g_s in this taxon. It is possible that the answer to the question of why ginkgo and other gymnosperms do not reduce the size and increase the number of their vascular bundles relates not to xylem but rather to phloem transport. Mechanical constraints derived from the role of the vascular bundles in stiffening the leaf blade are a second understudied possibility, with angiosperm fibers in major vein orders perhaps releasing minor vein vasculature to be optimized for purely hydraulic concerns.

THE POTENTIAL MITIGATION OF LOW VEIN DENSITY BY MESOPHYLL HYDRAULIC PROPERTIES

Returning to the apparent paradox with which we began, that vein density has a high explanatory power for variation in traits related to assimilation at coarse but not finer phylogenetic scales, can the preceding analysis offer a resolution? One possibility is that vein density is highly conserved, such that, even as variation in leaf expansion may tune the characteristic vein density for a given species to a particular microenvironment to some degree (Zwieniecki et al., 2004; Carins Murphy et al., 2014), interspecific variation in g_s at fine phylogenetic scales could be explained more by variation in r_m and r_V than D_v.

With respect to understanding the underlying material properties that contribute to variation in r_m/r_V, we know more about the dependence of vascular resistance on conduit geometry than about the dependence of r_m on tissue properties. For contributions to r_m from internal vapor transport, the volume of airspace within the mesophyll is the critical parameter (Rockwell et al., 2014a; Buckley et al., 2017). Yet for the liquid phase, whether flow through living cells occurs more through the wall space (apoplastic path) versus cell to cell across membranes (symplastic path as measured by the cell pressure probe, with plasmodesmata making an uncertain contribution; Kramer and Boyer, 1995) remains unresolved, meaning we do not know for certain which material properties drive r_m. Theoretical models have been employed to argue for the dominance of apoplastic flow (Buckley, 2015), but the scant available experimental evidence indicates similar conductivities for the symplastic and apoplastic paths of potato (*Solanum tuberosum*) parenchyma, and the symplastic path should then dominate transport based on its greater cross-sectional area (Michael et al., 1997). Estimates of cross-membrane hydraulic conductivities based on cell pressure probe measurements of membrane permeabilities also appear sufficient to explain whole-tissue conductances, without the need to invoke large apoplastic flows (Rockwell et al., 2014b).

To the extent that symplastic flow is important, r_m will be sensitive to cell size, as the number of membranes and cell walls crossed per unit length will contribute to mesophyll hydraulic resistivity. Interestingly, the mesophyll cells of ginkgo are elongate (~100 μm) in the intervein dimension, which may contribute to its low r_m relative to oak. In the case of cross-membrane

flow, the relevant measure of d/δ will be in terms of cell number rather than euclidean distance. Enlarged mesophyll cells could then partially mitigate large intervein distances, although at the cost of mesophyll surface area per cell volume, for which higher values allow greater chloroplast densities at the leaf level and so higher assimilation rates (Nobel, 2005). Thus, cross-membrane flows in the photosynthetic mesophyll set up an interesting tradeoff between water transport and carbon uptake. This tradeoff is expected to exist for the production and movement of carbohydrate from the photosynthetic mesophyll to the phloem, as gradients in sugar within the cytoplasm should be mitigated by cytoplasmic stirring, and the limiting step in transport is thought to occur across the plasmodesmata between cells (Liesche and Schulz, 2012). In this way, the high rates of gas exchange associated with a mesophyll with a large surface area-to-volume ratio may feed back on, or even drive, vein spacing. Thus, patterns suggestive of the conservation of cell number distances across different euclidean vein spacings may relate to sugar transport constraints rather than water.

An important influence of mesophyll cell length and number on the vein spacing observed for a particular leaf was suggested previously by Wylie (1939), who related closer vein spacing to relatively higher proportions of leaf cells elongate in the vertical (normal to the leaf surface) versus horizontal direction (e.g. spongy and epidermal versus palisade). The implication is that, over different euclidean vein spacings, cell number might be relatively conserved. Isolateral leaves with palisade differentiating toward both abaxial and adaxial surfaces have a large proportion of vertical tissue relative to bifacial leaves, a condition that Russin and Evert (1984) suggested could account for the dense vein spacing and small intervein distances observed in leaves of *Populus deltoides* ($D_v = 14.4\ \mathrm{mm}^{-1}$, $d = 55.6$). de Boer et al. (2016a) interpreted the closer vein spacing of isolateral versus bifacial eucalypts as a decrease in d/δ compensating for the increased δ of the former, resulting in a sacrifice in hydraulic optimality (Noblin et al., 2008) in support of higher transpiration and CO_2 uptake; to the extent that cell number is more relevant than euclidean distance, the loss of hydraulic optimality will be less. Aside from cell size and dimensions, other structural features of the mesophyll expected to contribute to a bulk-averaged r_m include the presence of branched sclereids (Brodribb et al., 2007), bundle sheath extensions (Armacost, 1944; Buckley et al., 2011), paraveinal mesophyll (Fisher, 1967), and extraxylery fibers (in *Gnetum gnemon*; Zwieniecki and Boyce, 2014b).

ALTERNATIVE CONSTRAINTS: STOMATAL STRUCTURE AND CELL SIZE

In positing a vascular or other hydraulic constraint on gas exchange, it is implicitly assumed that leaves are unconstrained by the maximum stomatal conductance they can achieve on an epidermal area basis. That is, if ferns, lycophytes, and gymnosperms were to increase the supply of water to the leaf epidermis, the assumption is that no other constraint would prevent them from increasing stomatal conductance and assimilation rates. We now consider the possibility of constraints arising directly from epidermal and stomatal architecture.

It has long been known that packing issues constrain stomatal index (the number of stomata per number of epidermal cells) within a given species (Salisbury, 1928). The one-cell-spacing rule between any two stomata, which may derive from requirements for solute reservoirs or potassium ion channel function, as well as space requirements for other cell types such as epidermal hairs (Bergmann and Sack, 2007; Papanatsiou et al., 2016) explain why stomatal index is more highly conserved between different environments than stomatal density (the number per unit area). As with increases in vein density, increasing stomatal density while holding stomatal size constant has a diminishing effect on total conductance, as the concentration gradients around each pore increasingly overlap (Ting and Loomis, 1965; Lehmann and Or, 2015). Increases in stomatal conductance, both within and across individual taxa, are then usually explained by both an increase in the number density and a reduction in the size of individual stoma (which reduces pore depth, thereby increasing conductance), with angiosperms achieving the highest densities and smallest stomata (Franks and Beerling, 2009; de Boer et al., 2016b; McElwain et al., 2016).

As with vein size and density, the question arises whether there exists a developmental constraint that prevents ferns and gymnosperms from simply reducing stomatal size and increasing density. One possible constraint could emerge from genome size, which is strongly associated with cell size in both animals and plants (Cavalier-Smith, 2005). The smallest angiosperm genome sizes are one order of magnitude smaller than those of gymnosperms or ferns, with the ancestral genome of angiosperms thought to be small (C-value less than 1.4 pg 1C; Leitch et al., 2005). While genome size is thought to respond to selective pressures on cell size (Cavalier-Smith, 2005), differences in epigenetic activities and mechanisms involved in purging long terminal repeat retrotransposons (Dolgosheina et al., 2008), as well as illegitimate recombination and genome fractionation and reduction following whole-genome duplication events, have been hypothesized to explain the restriction of the smallest genome sizes to angiosperms (Michael, 2014).

Stomatal cell size and genome size appear to be correlated in both eudicots and monocots (except tribe Poaceae; Hodgson et al., 2010), while across the angiosperms, epidermal cell size, guard cell length, and genome size are all correlated, with these traits negatively correlated with stomatal density (Beaulieu et al., 2008). In Figure 5, we plot guard cell area (from de Boer et al., 2016b) for angiosperms and gymnosperms for which we could find 1C DNA weights in a database maintained by the Kew Royal Botanic Gardens (Bennet and Leitch, 2012). The resulting data set, which must be

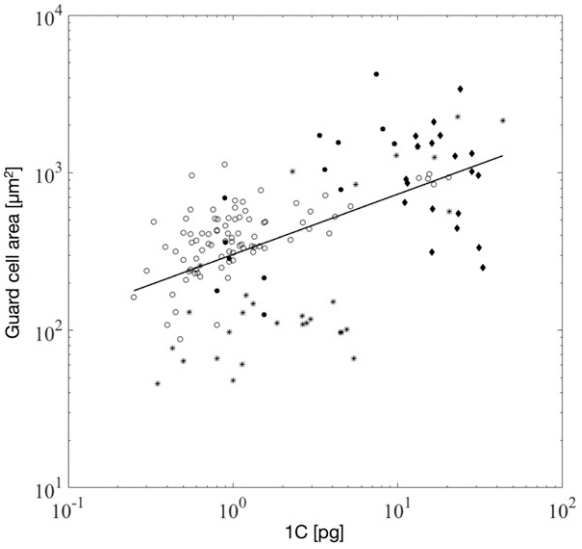

Figure 5. Guard cell area as a function of single-copy DNA weight across seed plants (n = 153, power law R^2 = 0.33), including basal angiosperms (black circles; n = 13, R^2 = 0.66), dicots (white circles; n = 84, R^2 = 0.37), monocots (asterisks; n = 30, R^2 = 0.57), and gymnosperms (diamonds; n = 25, R^2 = 0.07).

considered of lower quality because the stomatal and 1C data do not come from the same individuals or even the same collections of plants, confirms a relationship between stomatal and genome size across all seed plants and within dicots, basal angiosperms, and monocots, albeit weakly (Fig. 5).

As found by Hodgson et al. (2010), there was no obvious genome-stomatal size relationship in the Poaceae, which accounts for the dispersion in genome size for monocots around stomatal sizes on the order of 10^2 μm^2: this decoupling may be related to the characteristic dumbell shape of grass stomata (Esau, 1960; Chen et al., 2017), for which the relationship between pore length and cell size might be quite different. Within gymnosperms, there was no detectable relationship between stomatal and genome size, due to a large dispersion of stoma sizes over a more restricted range of genome sizes than seen in angiosperms. Yet, as with vein density, gymnosperms are clearly excluded from the space described by the smallest stomata and genomes sizes realized by some taxa in the core eudicots and monocots.

In addition to their potentially small size and high density, the qualitatively different functional characteristics of angiosperm stomata relative to earlier diverging vascular plants also may be important in the evolution of high leaf surface conductances. Specifically, angiosperm subsidiary cells (here defined functionally) give up considerable volume as guard cells swell, amplifying angiosperm aperture area for the same stomatal pore length by up to a factor of 2 compared with gymnosperms, ferns, and lycophytes (de Boer et al., 2016b). Subsidiary cell movement also may contribute to the greater aperture area per guard cell area achieved by angiosperms relative to ferns and lycophytes, which differ by a factor of 4 to 5 (Franks and Farquhar, 2007). However, there are potential costs. Due to the mechanical advantage subsidiary cells enjoy over guard cells, a local reduction in water potential leads to increasing stomatal aperture while a local gain in water potential leads to closure (Buckley, 2005). Such hydropassive wrong-way responses require metabolically active rectification to reverse, which appears to be governed by an abscisic acid-mediated pathway unique to angiosperms (Brodribb and McAdam, 2011; McAdam and Brodribb, 2016).

Yet, while the degree of mechanical advantage in early angiosperms appears to be understudied, it is notable that rates of stomatal conductance in this group, just as with vein density, are not noticeably high (Boyce et al., 2009; Feild et al., 2011b). Thus, while subsidiary cell volume loss does increase the maximum aperture for a given pore length, it would seem unlikely that selection for high g_s drove the evolution of mechanical advantage. Instead, in the context of the dark and disturbed hypothesis of angiosperm origins (Feild et al., 2004), subsidiary cell movement would be expected to improve the tracking of light flecks in an understory environment. This is because subsidiary cell movement is wrong way with respect to humidity shocks but right way with respect to light and thermal shocks. The increase in heat loading that accompanies a light fleck will push the transpiration rate higher and will, in the presence of subsidiary cells with mechanical advantage, set up a positive feedback on aperture to

OUTSTANDING QUESTIONS

- What is the relative importance of flow cell to cell across membranes versus through the wall space for the movement of water through the leaf mesophyll?
- Can estimates of the transport properties of living cells in planta, currently based on modeling to bridge the gap between equilibrium measurements of water potential and transpiration-induced gradients, be improved by cellular scale reporters of turgor or water activity?
- Would careful evaluation of the construction costs of vasculature in relation to transport capacity open a new window onto the impact of vessels and hierarchical reticulate leaf venation on maximum stomatal conductance?
- Do reductions in cell size across vascular, mesophyll, epidermal, and stomatal cells derive from episodes of genome reduction or follow the overcoming of diverse constraints in individual tissues?

contribute to faster opening in light (other things being equal) than the ion-mediated light response alone (Franks and Farquhar, 2007). Indeed, that such subsidiary cell hydropassive responses to E are, in general, faster than active ion-pump responses is demonstrated by the typical sequence in angiosperms of a wrong-way response followed by rectification (Buckley, 2005). A role for subsidiary cells in accelerating light responses could help explain why ferns and angiosperms respond to vapor pressure deficit at similar rates but angiosperms track light more efficiently (Lawson and Blatt, 2014).

In the same sense that the evolution of vessels and fibers in angiosperms may have been important for allowing more opportunistic and plastic growth forms in disturbed forest understories, and only later optimized to support high transpiration rates, the angiosperm stoma may then have evolved in response to a temporally heterogenous light environment, with its developmental potential for high fluxes only realized as the continued evolution of the vasculature allowed. In support of this idea, in a survey of the ANITA grade, the only taxa to achieve levels of $g_s > 400$ (comparable to high g_s in eudicots) were in Nymphaeales (Feild et al., 2011b). In this aquatic group, high stomatal density and small stomatal size co-occur with low vein densities. That such high densities and small stomatal sizes do not occur among terrestrial basal angiosperms returns us again to the idea of a vascular limitation in this group.

THE ANGIOSPERM ADVANTAGE: HIGHER FLUXES THROUGH MINIATURIZATION?

However, we have not landed precisely back where we started (see Outstanding Questions). From the perspective of both vascular and stomatal characteristics, the evolution of the capacity to support high leaf area-based fluxes appears to have involved a program of miniaturization across vascular, mesophyll, epidermal, and stomatal cell types, underscoring the potential significance of multiple episodes of genome reduction in angiosperms (Leitch et al., 2005). Given the differences between monocot and eudicot xylem and stomatal structure, this process likely proceeded independently in these two clades (Stevens, 2001).

In support of an integral role for cell size, work in the Proteaceae has shown that epidermal, mesophyll, xylem, and stomatal cell sizes tend to be correlated among themselves and inversely correlated with anatomical g_{max} and stomatal density (Brodribb et al., 2013). Further work in this group has shown that genome size is fairly stable within genera, with sister species showing much larger variation in stomatal size as a result of radiation into diverse environments, such that the genome-stomatal size (or genome-cell size) relationship admitted enough plasticity to vary between environments (Jordan et al., 2015).

Much of the scatter in the stomatal-genome size relationship could then reflect a tension arising from phylogenetic conservatism in genome size in conjunction with adaptive selection in stomatal (and cell) size that then feeds back to exert selective pressure on genome size over longer time scales (Hodgson et al., 2010). The relative weakness of vein density in predicting leaf hydraulic conductance at finer phylogenetic scales could arise from a similar conservatism in this trait, with adaptive radiations within genera tuning potentially intrinsic vein (r_V) and mesophyll hydraulic resistivity (r_m) or leaf thickness (δ) to balance the flux lost from stomata. Fully accounting for hydraulic and stomatal conductances in terms of mechanistic variables linked to well-defined material properties should help resolve these evolutionary patterns.

Supplemental Data

The following supplemental materials are available.

Supplemental Text S1. Derivations related to Equations 4 and 5.

ACKNOWLEDGMENTS

We thank three anonymous reviewers and the handling editor for comments and suggestions that greatly improved the analysis and article.

Received February 27, 2017; accepted June 13, 2017; published June 14, 2017.

LITERATURE CITED

Armacost RR (1944) The structure and function of the border parenchyma and vein-ribs of certain dicotyledon leaves. Proc Iowa Acad Sci **51:** 157–169

Beaulieu JM, Leitch IJ, Patel S, Pendharkar A, Knight CA (2008) Genome size is a strong predictor of cell size and stomatal density in angiosperms. New Phytol **179:** 975–986

Bennet MD, Leitch IJ (2012) Plant C-values Database, release 6.0. data.kew.org/cvalues/ (January 2017)

Bergmann DC, Sack FD (2007) Stomatal development. Annu Rev Plant Biol **58:** 163–181

Boyce CK, Brodribb TJ, Feild TS, Zwieniecki MA (2009) Angiosperm leaf vein evolution was physiologically and environmentally transformative. Proc Biol Sci **276:** 1771–1776

Brodribb TJ, Feild TS (2010) Leaf hydraulic evolution led a surge in leaf photosynthetic capacity during early angiosperm diversification. Ecol Lett **13:** 175–183

Brodribb TJ, Feild TS, Jordan GJ (2007) Leaf maximum photosynthetic rate and venation are linked by hydraulics. Plant Physiol **144:** 1890–1898

Brodribb TJ, Feild TS, Sack L (2010) Viewing leaf structure and evolution from a hydraulic perspective. Funct Plant Biol **37:** 488–498

Brodribb TJ, Holbrook NM (2003) Stomatal closure during leaf dehydration, correlation with other leaf physiological traits. Plant Physiol **132:** 2166–2173

Brodribb TJ, Holbrook NM (2005) Water stress deforms tracheids peripheral to the leaf vein of a tropical conifer. Plant Physiol **137:** 1139–1146

Brodribb TJ, Holbrook NM, Hill RS (2005) Seedling growth in conifers and angiosperms: impacts of contrasting xylem structures. J Bot **53:** 749–755

Brodribb TJ, Jordan GJ, Carpenter RJ (2013) Unified changes in cell size permit coordinated leaf evolution. New Phytol **199:** 559–570

Brodribb TJ, McAdam SA (2011) Passive origins of stomatal control in vascular plants. Science **331:** 582–585

Buckley TN (2005) The control of stomata by water balance. New Phytol **168:** 275–292

Buckley TN (2015) The contributions of apoplastic, symplastic and gas phase pathways for water transport outside the bundle sheath in leaves. Plant Cell Environ **38:** 7–22

Buckley TN, John GP, Scoffoni C, Sack L (2017) The sites of evaporation within leaves. Plant Physiol **173:** 1763–1782

Buckley TN, Sack L, Gilbert ME (2011) The role of bundle sheath extensions and life form in stomatal responses to leaf water status. Plant Physiol **156:** 962–973

Carins Murphy MR, Jordan GJ, Brodribb TJ (2014) Acclimation to humidity modifies the link between leaf size and the density of veins and stomata. Plant Cell Environ **37:** 124–131

Cavalier-Smith T (2005) Economy, speed and size matter: evolutionary forces driving nuclear genome miniaturization and expansion. Ann Bot (Lond) **95:** 147–175

Chen ZH, Chen G, Dai F, Wang Y, Hills A, Ruan YL, Zhang G, Franks PJ, Nevo E, Blatt MR (2017) Molecular evolution of grass stomata. Trends Plant Sci **22:** 124–139

de Boer HJ, Drake PL, Wendt E, Price CA, Schulze ED, Turner NC, Nicolle D, Veneklaas EJ (2016a) Apparent overinvestment in leaf venation relaxes leaf morphological constraints on photosynthesis in arid habitats. Plant Physiol **172:** 2286–2299

de Boer HJ, Eppinga MB, Wassen MJ, Dekker SC (2012) A critical transition in leaf evolution facilitated the Cretaceous angiosperm revolution. Nat Commun **3:** 1221

de Boer HJ, Price CA, Wagner-Cremer F, Dekker SC, Franks PJ, Veneklaas EJ (2016b) Optimal allocation of leaf epidermal area for gas exchange. New Phytol **210:** 1219–1228

Dolgosheina EV, Morin RD, Aksay G, Sahinalp SC, Magrini V, Mardis ER, Mattsson J, Unrau PJ (2008) Conifers have a unique small RNA silencing signature. RNA **14:** 1508–1515

Esau K (1960) Anatomy of Seed Plants, Ed 2. John Wiley & Sons, New York

Feild TS, Arens NC, Doyle JA, Dawson TE, Donoghue MJ (2004) Dark and disturbed: a new image of angiosperm ecology. Paleobiology **30:** 82–107

Feild TS, Brodribb TJ (2013) Hydraulic tuning of vein cell microstructure in the evolution of angiosperm venation networks. New Phytol **199:** 720–726

Feild TS, Brodribb TJ, Iglesias A, Chatelet DS, Baresch A, Upchurch GR Jr, Gomez B, Mohr BAR, Coiffard C, Kvacek J, et al (2011a) Fossil evidence for Cretaceous escalation in angiosperm leaf vein evolution. Proc Natl Acad Sci USA **108:** 8363–8366

Feild TS, Upchurch GR Jr, Chatelet DS, Brodribb TJ, Grubbs KC, Samain MS, Wanke S (2011b) Fossil evidence for low gas exchange capacities for early Cretaceous angiosperms. Paleobiology **37:** 195–213

Fisher DB (1967) An unusual layer of cells in the mesophyll of the soybean leaf. Bot Gaz **128:** 205–218

Franks PJ, Beerling DJ (2009) Maximum leaf conductance driven by CO_2 effects on stomatal size and density over geologic time. Proc Natl Acad Sci USA **106:** 10343–10347

Franks PJ, Farquhar GD (2007) The mechanical diversity of stomata and its significance in gas-exchange control. Plant Physiol **143:** 78–87

Gleason SM, Blackman CJ, Chang Y, Cook AM, Laws CA, Westoby M (2015) Weak coordination among petiole, leaf, vein, and gas-exchange traits across Australian angiosperm species and its possible implications. Ecol Evol **6:** 267–278

Hodgson JG, Sharafi M, Jalili A, Díaz S, Montserrat-Martí G, Palmer C, Cerabolini B, Pierce S, Hamzehee B, Asri Y, et al (2010) Stomatal vs. genome size in angiosperms: the somatic tail wagging the genomic dog? Ann Bot (Lond) **105:** 573–584

Horowitz P, Hill W (1989) The Art of Electronics, Ed 2. Cambridge University Press, New York

Jordan GJ, Carpenter RJ, Koutoulis A, Price A, Brodribb TJ (2015) Environmental adaptation in stomatal size independent of the effects of genome size. New Phytol **205:** 608–617

Kramer PJ, Boyer JS (1995) Water Relations of Plants and Soils. Academic Press, San Diego

Lawson T, Blatt MR (2014) Stomatal size, speed, and responsiveness impact on photosynthesis and water use efficiency. Plant Physiol **164:** 1556–1570

Lehmann P, Or D (2015) Effects of stomata clustering on leaf gas exchange. New Phytol **207:** 1015–1025

Leigh A, Zwieniecki MA, Rockwell FE, Boyce CK, Nicotra AB, Holbrook NM (2011) Structural and hydraulic correlates of heterophylly in *Ginkgo biloba*. New Phytol **189:** 459–470

Leitch IJ, Soltis DE, Soltis PS, Bennett MD (2005) Evolution of DNA amounts across land plants (Embryophyta). Ann Bot (Lond) **95:** 207–217

Liesche J, Schulz A (2012) In vivo quantification of cell coupling in plants with different phloem-loading strategies. Plant Physiol **159:** 355–365

McAdam SA, Brodribb TJ (2016) Linking turgor with ABA biosynthesis: implications for stomatal responses to vapor pressure deficit across land plants. Plant Physiol **171:** 2008–2016

McElwain JC, Yiotis C, Lawson T (2016) Using modern plant trait relationships between observed and theoretical maximum stomatal conductance and vein density to examine patterns of plant macroevolution. New Phytol **209:** 94–103

Michael TP (2014) Plant genome size variation: bloating and purging DNA. Brief Funct Genomics **13:** 308–317

Michael W, Schultz A, Meshcheryakov AB, Ehwald R (1997) Apoplasmic and protoplasmic water transport through the parenchyma of the potato storage organ. Plant Physiol **115:** 1089–1099

Nobel PS (2005) Physicochemical and Environmental Plant Physiology, Ed 3. Elsevier Academic Press, Burlington, MA

Noblin X, Mahadevan L, Coomaraswamy IA, Weitz DA, Holbrook NM, Zwieniecki MA (2008) Optimal vein density in artificial and real leaves. Proc Natl Acad Sci USA **105:** 9140–9144

Papanatsiou M, Amtmann A, Blatt MR (2016) Stomatal spacing safeguards stomatal dynamics by facilitating guard cell ion transport independent of the epidermal solute reservoir. Plant Physiol **172:** 254–263

Pittermann J, Sperry JS, Hacke UG, Wheeler JK, Sikkema EH (2005) Torus-margo pits help conifers compete with angiosperms. Science **310:** 1924

Rockwell FE (2010) Leaf water transport. PhD dissertation. Harvard University, Cambridge, MA

Rockwell FE, Holbrook NM, Stroock AD (2014a) The competition between liquid and vapor transport in transpiring leaves. Plant Physiol **164:** 1741–1758

Rockwell FE, Holbrook NM, Stroock AD (2014b) Leaf hydraulics. I. Scaling transport properties from single cells to tissues. J Theor Biol **340:** 251–266

Rockwell FE, Holbrook NM, Stroock AD (2014c) Leaf hydraulics. II. Vascularized tissues. J Theor Biol **340:** 267–284

Russin WA, Evert RF (1984) Studies on the leaf of *Populus deltoides* (Salicaceae): morphology and anatomy. Am J Bot **71:** 1398–1415

Sack L, Holbrook NM (2006) Leaf hydraulics. Annu Rev Plant Biol **57:** 361–381

Salisbury EJ (1928) On the causes and ecological significance of stomatal frequency, with special reference to the woodland flora. Philos Trans R Soc B **216:** 1–65

Scoffoni C, Chatelet DS, Pasquet-Kok J, Rawls M, Donoghue MJ, Edwards EJ, Sack L (2016) Hydraulic basis for the evolution of photosynthetic productivity. Nat Plants **2:** 16072

Sperry JS, Hacke UG, Oren R, Comstock JP (2002) Water deficits and hydraulic limits to leaf water supply. Plant Cell Environ **25:** 251–263

Sperry JS, Hacke UG, Wheeler JK (2005) Comparative analysis of end wall resistivity in xylem conduits. Plant Cell Environ **28:** 456–465

Sperry JS, Love DM (2015) What plant hydraulics can tell us about responses to climate-change droughts. New Phytol **207:** 14–27

Stevens PF (2001) Angiosperm Phylogeny Group Website. http://www.mobot.org/MOBOT/research/APweb/

Ting IP, Loomis WE (1965) Further studies concerning stomatal diffusion. Plant Physiol **40:** 220–228

Woodruff DR, Meinzer FC, Lachenbruch B (2008) Height-related trends in leaf xylem anatomy and shoot hydraulic characteristics in a tall conifer: safety versus efficiency in water transport. New Phytol **180:** 90–99

Wylie RB (1939) Relation between tissue organization and vein distribution in dicotyledon leaves. Am J Bot **26:** 219–225

Zhang YJ, Rockwell FE, Graham AC, Alexander T, Holbrook NM (2016) Reversible leaf xylem collapse: a potential "circuit breaker" against cavitation. Plant Physiol **172:** 2261–2274

Zhang YJ, Rockwell FE, Wheeler JK, Holbrook NM (2014) Reversible deformation of transfusion tracheids in Taxus baccata is associated with a reversible decrease in leaf hydraulic conductance. Plant Physiol **165:** 1557–1565

Zwieniecki MA, Boyce CK (2014a) Evolution of a unique anatomical precision in angiosperm leaf venation lifts constraints on vascular plant ecology. Proc Biol Sci **281:** 20132829

Zwieniecki MA, Boyce CK (2014b) The role of cellulose fibers in *Gnetum gnemon* leaf hydraulics. Int J Plant Sci **175:** 1054–1061

Zwieniecki MA, Boyce CK, Holbrook NM (2004) Hydraulic limitations imposed by crown placement determine final size and shape of *Quercus rubra* L. leaves. Plant Cell Environ **27:** 357–365